npj | urban sustainability

Article

Published in partnership with RMIT University

https://doi.org/10.1038/s42949-026-00381-6

Urban agrivoltaics enhance crop resilience and food-energy synergies in a changing climate

Check for updates

Caroline Merheb[1], Joshua S. Caplan[2], Pralad Phuyal[1], Jordan Macknick[3], Nicholas C. Davatzes[1] & Sujith Ravi[1] ✉

Urban agrivoltaics, the synergistic integration of solar photovoltaics with urban agriculture, offers a transformative solution to food and energy insecurity, which are major barriers to sustainable urban development, especially in low-income urban areas facing intensified heat and water stress due to climate change. With 70% of the global population projected to live in cities by 2050, maximizing underutilized urban spaces is critical. Our study presents the first evaluation of ground-based agrivoltaics in an urban context, demonstrating that, while early-season yields may decline due to light reduction in temperate climates, productivity rebounds during periods of extreme heat, extending harvest windows and enhancing crop resilience. As cities seek climate-adaptive infrastructure, converting just a fraction of vacant land and rooftops to urban agrivoltaics can yield significant co-benefits such as generating renewable energy for thousands of households while supplying fresh produce to help alleviate food deserts.

Food insecurity, which is strongly correlated with income poverty, remains a major impediment to sustainable urban development, especially due to the restricted availability of fresh produce[1]. In particular, food availability is constrained by high transportation costs, policy and regulatory barriers, infrastructure challenges, seasonal limitations, and climate variability[2]. These issues exacerbate social, economic, and racial inequities[3], contributing to serious health problems, especially for children[4,5]. Moreover, the high cost of fresh produce often leads to unhealthy dietary patterns, marked by a high intake of ultra-processed foods and limited physical activity, resulting in widespread malnutrition[6]. With urban populations projected to reach 70% of the global total by 2050[7], urban agriculture is increasingly recognized as a strategy to enhance food resilience, community health, and environmental sustainability, primarily by strengthening the local supply of fresh produce[8–10]. Additionally, urban agriculture supports the pollination networks that are essential for crop productivity[11] and helps mitigate carbon emissions, directly through photosynthesis and indirectly by promoting less carbon-intensive diets[12]. However, urban agriculture is vulnerable to intensifying climate extremes, such as prolonged heat waves and droughts[13], which impair photosynthesis[14] and reduce yields[15–17].

Compounding these risks, urban heat island effects, driven by anthropogenic activity[18] and exacerbated by climate change[19] lead to severe health impacts, increased mortality rates[20], and rising electricity demand[21]. Food and energy poverty often occur in the same areas within cities, further complicating food distribution and storage, particularly when refrigeration is required. Moreover, continued reliance on fossil fuels runs counter to the United Nations Sustainable Development Goals[22] and intensifies environmental and public health burdens[20]. In this context, urban agrivoltaics (UrAV),the co-location of food and solar energy production on urban land such as rooftops and vacant lots,offers a promising solution by enhancing land-use efficiency[23–29], while simultaneously addressing food and energy security in rapidly growing cities.

From a food production perspective, UrAVs, like other forms of agrivoltaics, can protect plants from excessive heat and moisture loss by reducing exposure to high-intensity solar radiation[28,30,31]. Changes in the microclimate under solar photovoltaics (PV), such as lower air temperature and higher relative humidity, can also reduce heat and drought stress and improve water use efficiency[30,32,33]. Field experiments on agrivoltaics have reported improved yields under PV panels compared to full sun conditions, particularly during hot periods[34]. However, yield and microclimatic changes are not only influenced by climate, but also by the site size, geographic location, crop types, and design of the PV system, including the technology, layout, spacing, and height of panels[34–38]. Prior studies of agrivoltaics systems in temperate climates, which have mainly addressed monoculture farming in systems greater than 500 m^2, have reported both higher[28,39,40] and lower[28,32,39,41–48] yields compared with controls, with gains most often reported for leafy vegetable crops[40]. Yield reductions have been primarily

[1]Department of Earth & Environmental Science, Temple University, Philadelphia, PA, USA. [2]Department of Architecture & Environmental Design, Temple University, Ambler, PA, USA. [3]National Renewable Energy Laboratory, Strategic Energy Analysis Center, Golden, CO, USA. ✉e-mail: sravi@temple.edu

attributed to using shade-intolerant crops (e.g., corn, rice, barley, beans, potatoes, grapes) together with low-transparency PV panels in row-crop agriculture[32,42,44,46,47]. It has been shown that decreasing shade coverage (e.g., by increasing the spaces between neighboring panels) can reduce losses[45] and even produce greater yields than crops grown in full sun conditions[39]. An alternative approach to increasing yields by allowing solar radiation penetration is to employ solar tracking systems instead of fixed PV panels[28,41] or using semi-transparent PV panels. However, in the context of urban land scarcity, large solar infrastructure and solar tracking are likely to be impractical and excessively expensive[38].

In urban communities, agrivoltaic systems offer a promising approach to enhancing resilience by increasing access to renewable energy and affordable, nutritious food, particularly for vulnerable populations. Despite growing interest, to our knowledge, no study has comprehensively evaluated the performance of agrivoltaic systems specifically designed for urban environments in temperate climates. Here, we compare the food production of such a system to that of a control garden in the U.S. Mid-Atlantic region and examine associated physiological, morphological, and nutritional differences in the crops. More broadly, we aim to inform urban farmers, policymakers, and planners about means of enhancing food production through agrivoltaics in order to advance broader goals such as reducing food insecurity, improving access to clean energy, and fostering inclusive community spaces. This research is critical because successful implementation can increase public acceptance of agrivoltaic technologies and support the development of scalable, cost-effective solutions that contribute to urban sustainability[49,50].

Results

Crop-specific spatiotemporal variability in yields

All crops except for Stringless bush beans and both radish varieties experienced yield reductions in the agrivoltaics site when summed across the growing season ($p < 0.001$ pooled together and $p < 0.1$ separately; Supplementary Table 1), though there was considerable variation in the magnitude of reduction across crops. At the extremes, Genovese basil had 40% loss whereas Stringless bush beans had no loss (Fig. 1c). Further, some varieties had smaller losses compared to their peer varieties, such as Sungold tomatoes, Stringless bush beans, Red salad bowl lettuce, and Donato radishes (by 8%, 38%, 21%, and 12%, respectively). Despite these losses, certain crops like Stringless bush beans (+18%), Red salad bowl lettuce (+23%), and Donato radishes (+25%) had higher yields in specific subplots of the agrivoltaics site, especially those on the south, east, and west edges (Fig. 1a, b), where transmitted light was higher than in other subplots (>60% and >40% of transmitted plus diffuse light at 2 m and 0.7 m heights, respectively[51]).

Yield reductions were greatest early in the growing season, but compensation occurred during a prolonged hot and dry period later in the season (Fig. 1d and Supplementary Fig. 1). Environmental data indicated that Donato radish, both lettuce varieties, both bush bean varieties, and Genovese basil thrived in high-light, mild-temperature conditions (Fig. 2a–c, e *solid boundary*). During the hot/dry period in late summer and fall, these crops, along with Stringless bush beans, were harvestable only in more shaded subplots (Fig. 2a–c, e *dotted boundary*). Cherry tomato yield was largely unaffected by environmental conditions, but some plants had delayed development (Supplementary Fig. 1; 100% change, implying no harvestable plants), and this impacted later yields in certain subplots.

Overall, yields were optimal in plots whose light transmittance at the sun's peak exceeded 52%. Crop yield also depended on the time of day during which a plot received moderate light intensities, which was related to the elevation and the direction of the sun. For instance, lettuce and radishes were more productive on the eastern side of the AV site, which is exposed to morning sunlight, while bush beans were more productive on the southwest side, which is exposed mostly to afternoon sunlight. On the other hand, basil was most productive on the northwest side of the site, where late afternoon sunlight was prominent. In addition, cherry tomatoes were most productive on the southern side of the site, which is more shaded in the morning and late afternoon but receives more radiation during midday.

Microclimatic and biotic factors influence early crop development

The height of bush bean plants (measured 3–4 weeks after seeding) varied spatially within the agrivoltaics site (Fig. 3a). On average, plants were 3 cm taller in the control site, while those in plots with ~75% of transmitted light were an additional 3 cm taller. Thus, height decreased with reduced light transmission, consistent with previous studies[32]. Similarly, bush bean yield was reduced in the agrivoltaics site where light was low, but particularly at the beginning of the growing season when temperature was also low (Fig. 2c *solid boundary*). This suggests that growth was delayed and/or flowering was reduced, as reported by other studies[32,43,52]. Another challenge bush beans faced was an outbreak of Mexican bean beetle (*Epilachna varivestis*) in July, causing a disproportional loss of leaf area for plants in the agrivoltaics site (Supplementary Fig. 2a).

The volume of radish roots (Fig. 2a) and the size (i.e., area) of lettuce leaves (Fig. 2b) were smaller in the agrivoltaics site, where there was more soil moisture and shade. Also, specific leaf area (SLA) significantly differed between lettuce varieties at both sites ($p < 0.17$; Supplementary Table 1), increasing with the intensity of shade (Supplementary Fig. 2b), consistent with previous studies[41,45]. The increase in SLA for leaves juxtaposed with higher yields in these shaded regions, as was found for radish leaves early in the season, when low temperatures were more prevalent ($p < 0.15$; Supplementary Fig. 3 and Table 1). With the intensification of heat through the growing season, the yield of radish leaves became greater in less shaded plots of the agrivoltaics site. This was exacerbated by mice, which appeared to prefer feeding on shaded radish leaves. For cherry tomatoes, fruit sizes exhibited wide variation at both sites, but there was no discernible association between fruit size and environmental conditions (Fig. 2d). The high variation may relate to the indeterminate growth habit (and therefore large size) of these varieties, since it leads to variability in light transmittance along their stems.

Basil grown in the agrivoltaics site had more harvestable plants in subplots with low light transmittance (0.2–0.4 on the normalized scale) during hot periods than subplots in the control site that were shaded by neighboring plants but had higher light transmittance (>0.4) for moderate temperatures (Fig. 2e). Overall, the number of harvestable basil plants was lower under agrivoltaics, as germination was delayed in highly shaded areas, resulting in less mature plants. Nonetheless, SLA was greater for these plants ($p = 0.04$; Supplementary Table 1), especially in subplots exposed to more light in July and September and in more shaded subplots in August, when air temperature was at its peak (Fig. 3b). Accordingly, the abundance of light in July and September led to more rapid development and growth and, thereby, higher SLA. However, in August, increased shading in the agrivoltaics site reduced heat stress compared to plants grown in full-sun, thus triggering leaf acclimation strategies including leaf expansion and the development of thinner (i.e., higher SLA) leaves to maximize light capture[53]. Notably, basil's SLA in September was significantly reduced in the agrivoltaics site, likely not due to the direct effect of shading on growth, but, rather, due to heavy herbivory by Mexican bean beetles (Supplementary Fig. 4).

Several of the aforementioned responses to growth in the agrivoltaics site were also reflected in dry weights. Like SLA, the dry weight of basil leaves was significantly greater in the agrivoltaics site (Fig. 3d) ($p < 0.001$; Supplementary Table 1). Additionally, bush beans were not only taller in the control site but also had greater leaf dry weights than those grown under agrivoltaics ($p < 0.026$; Supplementary Table 1). However, despite the size variations noted above (Fig. 2), there were no significant differences between agrivoltaic and control for dry weights for Buttercrunch lettuce (leaves), either cherry tomato varieties (fruits), Donato radishes (roots), or Contender bush beans (fruits), but there were differences for Stringless bush beans (fruits), Red salad bowl lettuce (leaves), and French breakfast radishes (roots; $p < 0.08$), (Fig. 3c, d) ($p > 0.2$; Supplementary Table 1).

Shade acclimation vs light limitation in agrivoltaics plants

Electron transport rate (ETR), an indicator of the light reactions of photosynthesis, was investigated both in terms of rates that leaves

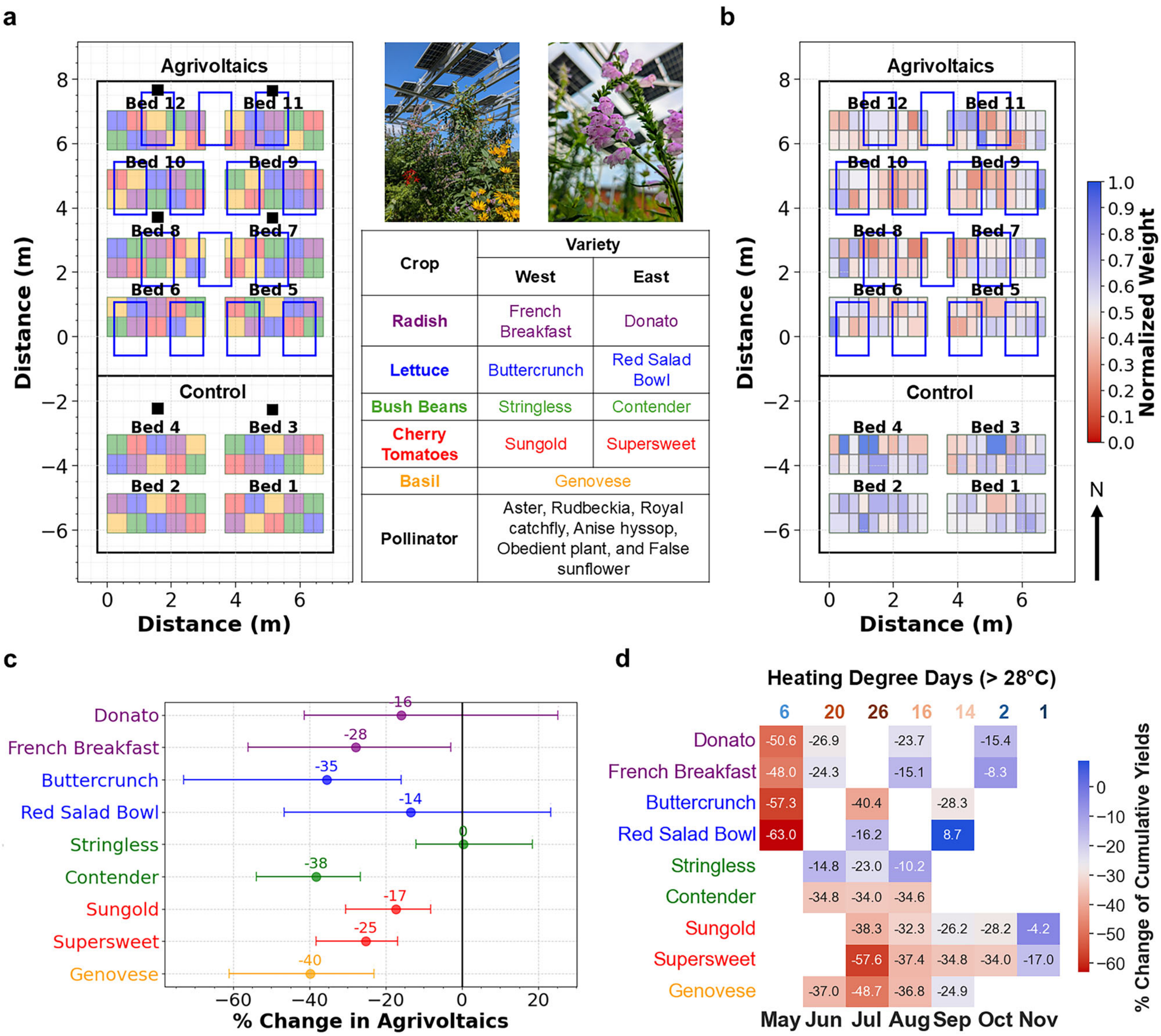

Fig. 1 | Experimental design and spatiotemporal changes in yield. **a** Overview of the urban agrivoltaics site in Ambler, Pennsylvania, USA, **b** spatial distribution of normalized cumulative yield (summed across all 2024 harvests), **c** cumulative difference in yield for the full growing season between agrivoltaics and control settings, and **d** monthly differences in yield with heating degree days also shown (i.e., the number of days in a month where the maximum temperature exceeded 28 °C). Yield differences were calculated as the difference between agrivoltaics and control yield (measured as fresh weight) relative to control yield. Negative and positive values indicate yield losses or gains in the agrivoltaics site, respectively. For **b**, the normalized weight was computed by dividing the cumulative yield weight from every subplot within each crop variety by the maximum cumulative weight from all subplots. For **c**, the cumulative weight from each subplot in the agrivoltaics site was computed for each crop variety and then paired with the average cumulative weight from all subplots in the control to determine the minimum, average, and maximum differences. For **d**, the cumulated weights were computed from the average weights for each site (control vs. agrivoltaics), harvest month, and variety.

were capable of achieving under standardized conditions, as well as rates achieved when grown in ambient conditions. In three of the five varieties evaluated, the presence of solar panels reduced the maximum ETR plants could reach at high irradiance (i.e., curves in Fig. 4). This demonstrates that they experienced shade acclimation through an adjustment in their leaf construction; this was also reflected in greater SLA, as noted previously. However, acclimation was not observed in Donato radish or Genovese basil.

ETR measured under ambient conditions was reduced in all seven of the varieties tested (i.e., points in Fig. 4). However, the size of realized ETR reductions differed strongly among varieties, with smaller shifts for Stringless bush beans, Supersweet cherry tomatoes, and Red salad bowl lettuce and larger shifts for Donato radishes, Buttercrunch lettuce, Genovese basil, and Sungold cherry tomatoes. In conjunction, the lettuce and bush bean varieties with smaller differences in ETR also exhibited lower yield reductions (and, in some cases, yields were greater than in control plots). These crops, in addition to radishes and basil, had lower peak ETR and higher production in the agrivoltaics site (Supplementary Fig. 1; between August and September).

Realized ETR corresponded reasonably closely to ETR measured in light response curves, though there were some discrepancies. These were likely due to differences in the microclimatic conditions under which they were measured. In particular, the instrument used for light response curves imposed somewhat cooler leaf temperatures (often 3–5 °C) than the ambient conditions under which realized ETR was measured.

Agrivoltaics benefits (micro) nutrient concentrations

Although micronutrient (B, Fe, Mn, Cu, Zn, and Al) concentrations varied by setting for several elements ($p < 0.088$; Fig. 5 and Supplementary Table 1),

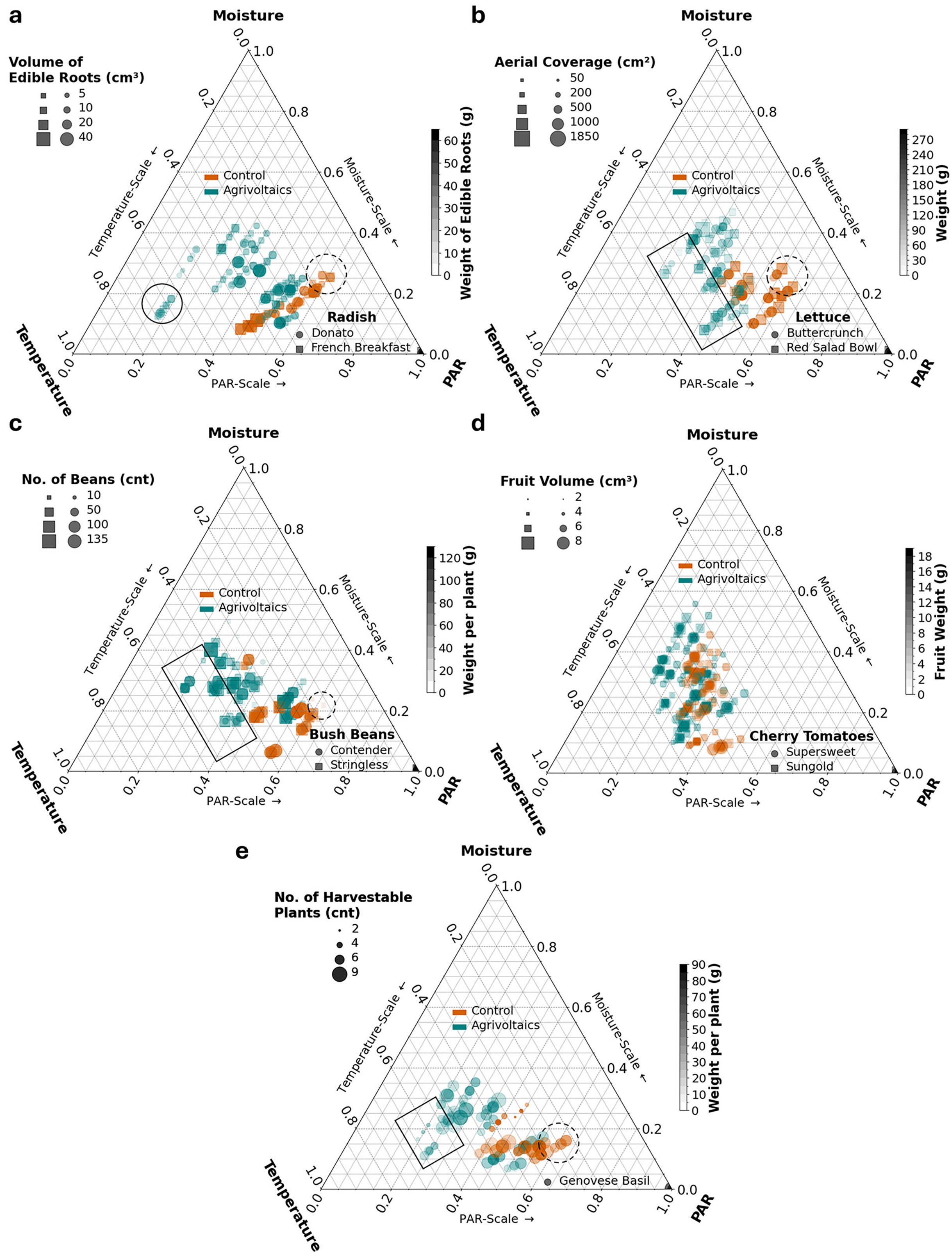

Fig. 2 | Crop yield and morphology across temperature–light–moisture gradients. Yield (measured as fresh weight) and morphological features of **a** radishes, **b** lettuces, **c** bush beans, **d** cherry tomatoes, and **e** basil in agrivoltaics and control sites together with environmental conditions (soil moisture, ambient air temperature, and photosynthetically active radiation, PAR; see Supplementary Notes for details).

they typically remained within healthy ranges for both the agrivoltaics and control settings. Exceptions included deficiencies in B, Fe, and Al for cherry tomatoes, deficiencies in Mn and Al for bush beans, and surplus in Fe and Al for basil (Supplementary Table 2). Overall, though, plants grown under agrivoltaics had smaller deficiencies (−25%) than those within the control (−50% to −75%) (Fig. 5).

For macronutrients (N, P, Mg, K, and Ca), concentrations were generally within healthy ranges in both agrivoltaics and control settings,

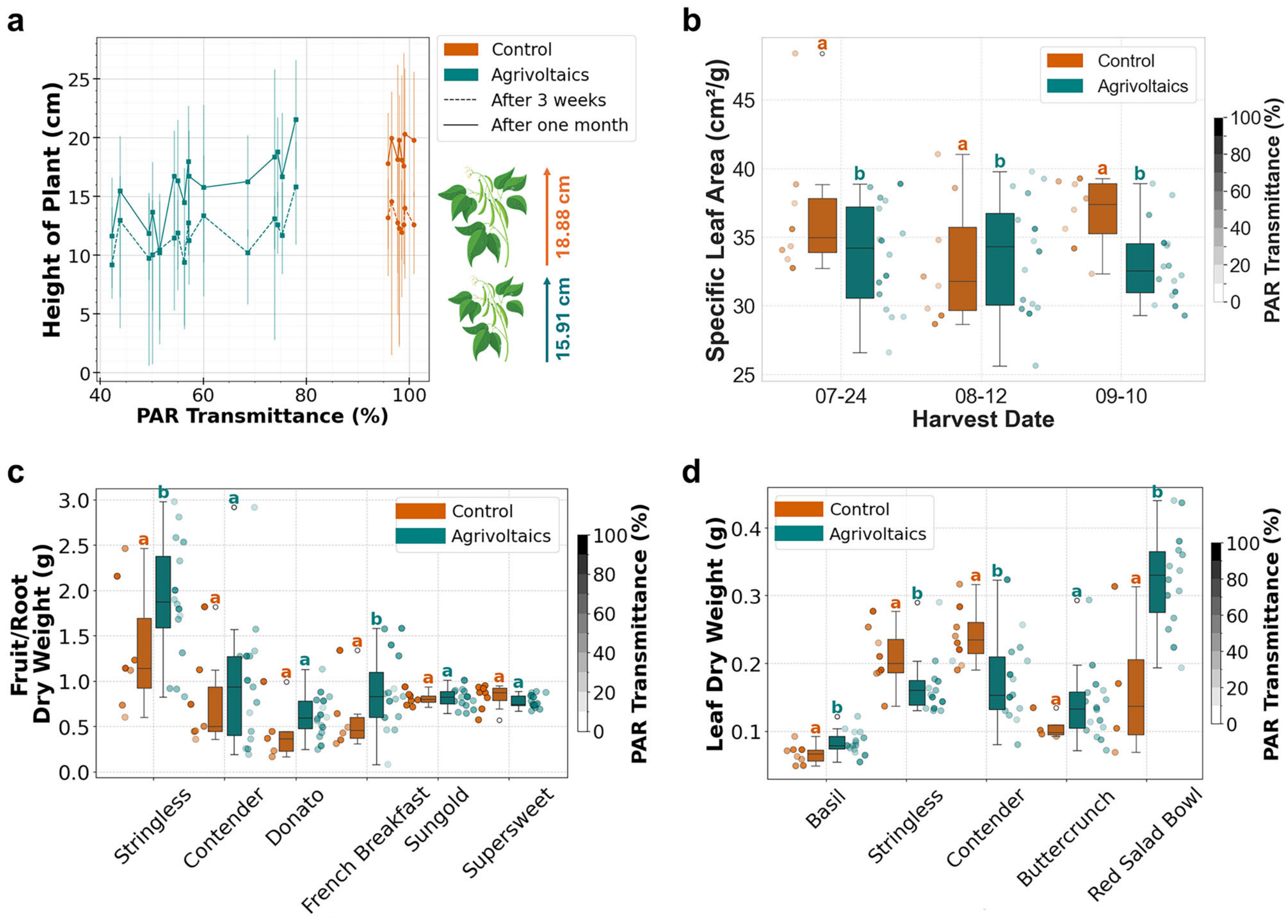

Fig. 3 | Effects of light transmittance on crop height, leaf traits, and biomass. **a** Average height (±SE) of beans in each subplot. **b** Specific leaf area (SLA) of basil measured at different harvest dates for all subplots. Dry weight of individual fruits **c** and leaves **d** for all subplots. Each subplot corresponds to a unique PAR (photosynthetically active radiation) transmittance around noon.

although there were some exceptions. Both sites exhibited surpluses of P, Mg, K, and Ca in basil, P and K in lettuce, P in bush beans, and P, K, and S in radishes (Supplementary Table 3). Further, there were reductions in N, Mg, Ca, and S for all crops except basil. When compared to full sun environments (i.e., the control site), nutrient concentrations were lower for cherry tomatoes (−25% to −75%) and radishes (−25% to −50%) in the agrivoltaics site (Fig. 5). However, losses were reduced in shaded lettuces and bush beans, which underwent leaf building responses to lower light conditions. For all crops, agrivoltaics subplots with low light transmittance had higher N concentrations (0 to +25%) and lettuce and bush beans had higher concentrations of all nutrients (>+25%).

Discussion

In other studies of crop-based agrivoltaic systems conducted in temperate climates, yield reductions were often lower than those observed in our study (Supplementary Table 4). This is likely because those studies focused on large-scale systems featuring taller and more widely spaced PV panels, which would have allowed greater light transmittance and thereby supported more rapid photosynthesis[32,40–44,46]. Photosynthesis is directly correlated with plant growth and increases with air temperature, transmitted light, and soil moisture content until reaching saturation points, beyond which the rate declines[54,55]. At the beginning of the growing season, when daylength and temperature were sufficient for the crops we used[30], the combination of reduced light due to shading and lower temperature likely reduced photosynthesis rates[56], delaying maturation, and ultimately causing reductions in yield[57]. Lower temperatures may have also delayed germination (Supplementary Figs. 5 and 6c)[56] (see Supplementary Notes for ways to improve seed vigor). Likewise, low light and moderate temperatures may have delayed root system development, resulting in smaller plants[58] (Figs. 3 and 4) and restricted flower production (Supplementary Fig. 6a, b). Reduced root system development may have slowed nutrient uptake rates[56], impacting the structural makeup of proteins, nucleic acids, chlorophylls, certain secondary metabolites, and defense-related micro- and macromolecules[56,59]. However, the structural and functional symptoms and disruptions imposed by nutritional losses from our site were likely suppressed in shaded crops by gains in other elements and through morphological and physiological changes, while counteracting those initially suppressed[60,61]. Fortunately, despite some reductions, micronutrient concentrations in the agrivoltaic site remained within healthy ranges, avoiding metal deficiencies or toxicities[62–65] (Supplementary Table 2).

Nonetheless, reduced light conditions (as low as 40% transmittance) in the agrivoltaics site exerted a beneficial effect during the hottest part of the growing season, alleviating physiological stress from prolonged exposure to intense radiation. More specifically, shade would have reduced the sensible heat flux (direct sunlight + air convection) regardless of the extent of air cooling in the agrivoltaics. Such a change in the microclimate can induce plants to increase in height, stem diameter, lateral branch length, leaf mass, and leaf number compared to full sun, improving yields and creating an environment enabling more efficient harvesting. Another effect of shade is that basil seeds experienced a longer dormancy in the agrivoltaics, though they were able to germinate when temperatures became warmer; shade also provided ongoing productivity through high heat events, even when plants in full-sun went dormant (Supplementary Fig. 6c). Finally, lettuces and radishes, which were seeded at multiple stages of the growing season, had

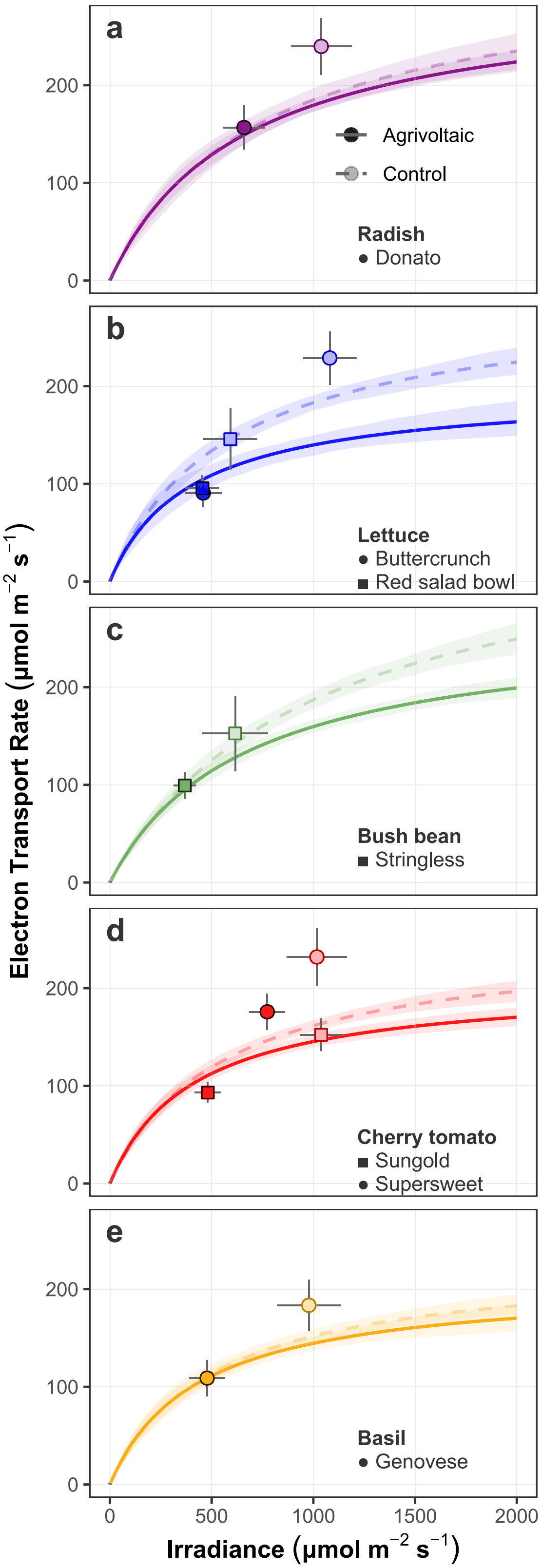

Fig. 4 | Photosynthetic activity of crops. Electron transport (ETR, a measure of photosynthetic activity) of **a** radish (Donato only), **b** lettuces, **c** bush beans (Stringless only), **d** cherry tomatoes, and **e** basil vs. incident irradiance in agrivoltaics and control sites. Curves are rectangular hyperbolic functions (Eq. 29 from[71]) fitted to light-response data measured with an LI-6800F; shaded regions are 95% confidence intervals. Points with error bars depict realized ETR rates (mean ± SD), which were measured under ambient conditions with an LI-600. Data shown are pooled across sampling dates.

greater germination rates in the agrivoltaics between June and August (Supplementary Fig. 5), likely due to relief from heat stress.

Food production at our agrivoltaics site could likely be enhanced by adopting strategic bed layouts, reducing irrigation, and minimizing shading from tall plants. For instance, overlapping high-performance regions with adequate soil moisture availability, the raised beds could be installed in a U shape (Supplementary Fig. 7). Other designs could also be adopted in cities to enhance the esthetics of empty spaces or rooftops, such as using a dome design and overlaying spiral structures for elevated crops and placing flower beds between them (Fig. 6b). Moreover, PV structures could reach full coverage if different panel technologies were used (e.g., bifacial semi-transparent/high efficiency or transparent/low efficiency) and if coated with highly reflective material. This would ease rainfall collection and enhance diffusivity and transmittance of light while maintaining a palatable energy production and avoiding the high costs of land conversion to agriculture (Fig. 6c). Another option would be to add LEDs beneath the PV array to increase transmitted light[34] as this was shown to increase the carbon acquisition of shaded plants during high heat periods (Fig. 4).

Even with our current design, the improvement in yields later in the growing season would have made UrAV financially competitive with an urban farm without PV. Profits per subplot ($0.6 \times 0.6\,m^2$) from UrAV ranged between \$17 and \$164 while losses ranged between \$46 and \$418 (Supplementary Table 5 and Fig. 8). In all cases, these deficits would have been fully compensated for by energy production in 4 months, meaning the remaining 8 months in the year would have yielded additional profit (Supplementary Table 6). Further, our UrAV site had a Land Equivalent Ratio of 1.3 (Supplementary Table 7), meaning a land-use efficiency of 130%. In other words, co-location would have avoided 30% of the land cost needed for to generate food and solar energy separately, which is consequential given that urban spaces are expensive and vacancies are limited. Furthermore, our experiment indicates that UrAVs can extend the growing season, enabling multiple cycles of leafy vegetables to be grown even when conditions outside the system are unfavorable. UrAV can thus contribute to higher yields, especially for crops minimally affected by the reduced light regime, since off-season produce can command higher market prices. Fortunately, small-scale urban farms often prioritize winter leafy vegetables (e.g., lettuce and spinach) or short-duration crops (e.g., radish and bok choy) due to their ability to yield multiple harvests, at least when there is high demand locally.

In addition to financial profits, UrAVs can improve food and energy security for people who have limited access to fresh produce and are vulnerable to paying electricity bills due to low income. While some cities, such as Philadelphia, are attempting to reduce food deserts by promoting gardening (Fig. 6a), the UrAV strategy additionally provides a means of shielding crops from natural and anthropogenic heat. Moreover, converting 28% of the vacant land and building rooftops in Philadelphia to UrAV would be sufficient to meet electricity demand for at least as many households (+11,600) as there are in food deserts (Fig. 6a). Further, these UrAV sites, which span over 80% of the food deserts, could supply these neighborhoods with fresh produce throughout an extended growing season amenable to both cool season and warm season crops. Further, these systems may not only mitigate urban heat islands with increased crop cover[66], but also can provide shields against summer heat for urban growers in these neighborhoods, of which ~93% are located in heat-vulnerable tracts (Fig. 6a). Nonetheless, investing in UrAVs elucidates financial and transit access to fresh vegetables, creates decentralized energy production systems that support the grid, generates multi-disciplinary employment, and improves land value. Finally, UrAVs would help to protect a sensitive portion of the population (children and elderly people), who are more prevalent in these neighborhoods[67], by mitigating poor nutrition and reducing overheating from lack of air conditioning (AC) during high heat events[68,69]. Fortunately, peak heat events are juxtaposed with peak solar generation, making it possible to meet AC demand, which would also reducing the incidences of tapping into hydrants.

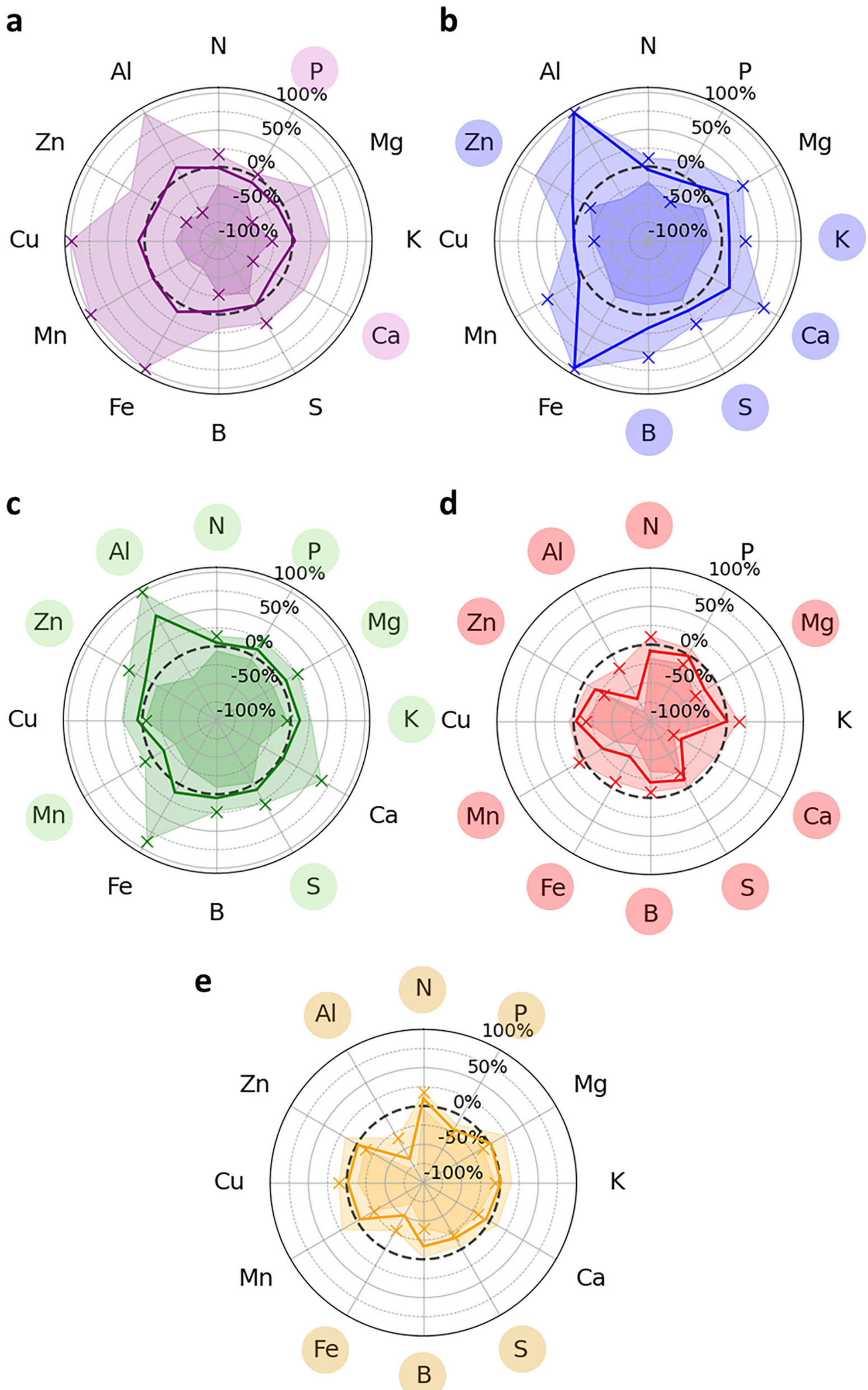

Fig. 5 | Elemental concentration changes in crops. Change in tissue elemental concentrations ([Agrivoltaics-Control]/Control, as %) in crops (**a** radish, **b** lettuce, **c** bush beans, cherry tomatoes, **e** – basil), where the average value from the control was used in combination with the average, minimum, and maximum values from the agrivoltaics site. The solid line shows the average change, while the dark and light filled boundaries show the extent of minimum and maximum changes, respectively. Negative and positive values thus indicate losses and gains of these elements in the agrivoltaics site, respectively. Crosses depict the location of shaded subplots; if it is located on the minimum boundary, shading resulted in the lowest change, and if it is on the maximum boundary, shading resulted in the highest change. Colored circles behind element labels indicate statistically significant differences.

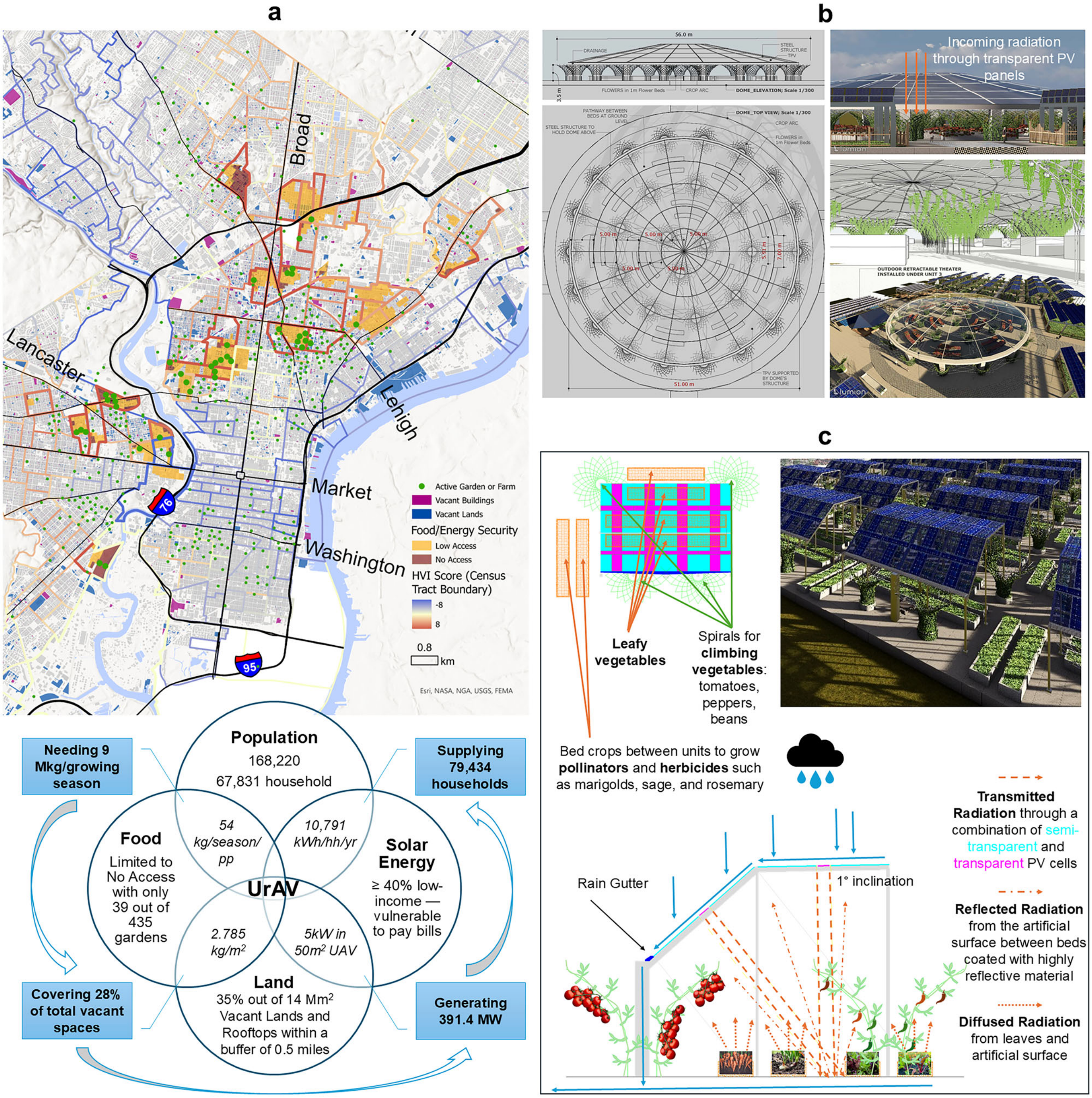

Fig. 6 | The potential of urban agrivoltaics to mitigate food and energy security in low-income neighborhoods and improve the esthetics of cities. **a** Map of the census tracts in Philadelphia that are both low-income (40% or more people below the poverty line) and have limited to no access to food; heat vulnerability index (HVI) of tracts is also shown. Negative and positive HVI scores refer to low and high levels of vulnerability to heat, respectively. The shapefiles for HVI, gardens, access to food, vacant lots, and buildings were obtained from OpenDataPhilly. Data on the population were extracted from census data (https://data.census.gov/profile/Philadelphia_city,_Pennsylvania?g = 160XX00US4260000). The diagram represents a summary of the analysis on how many urban agrivoltaics sites (similar in size to that used in this study, 50 m^2) can be installed in vacant land and on rooftops to support homes with limited access to food and energy, which are not supported by the existing number of gardens and farms and the economic status, respectively. **b**, **c** are illustrations of urban agrivoltaics designs that can be used to improve esthetics, transmitted radiation, and water management. These drawings were extracted from the winning project (The MUUSEculture Garden; The Girl from the Never Mountains Team; designed by C. Merheb – First Author) in the student competition for urban agrivoltaics designs in the 2024 Agrivoltaics World Conference.

This study was conducted in a temperate climate, where urban agriculture remains prominent. However, we anticipate that the benefits of urban agrivoltaics would be even greater in arid cities experiencing more severe water stress and heat island effects. Further research across diverse agroclimatic zones is needed to fully evaluate co-benefits, particularly the impacts of crop cooling on panel temperature and electricity generation. Additionally, while reduced heat stress is a benefit to crops during hot periods, it may also attract pests. We observed that Mexican bean beetles preferentially damaging bush beans and then basil under panels. Conversely, improved microclimates may support pollinators, which appeared more active within agrivoltaic sites, offering additional ecological and human health advantages. Further studies are required to monitor pollinator activity and human activity in the altered working conditions to better understand these synergies and tradeoffs.

Although urban agrivoltaic systems face challenges associated with their small scale and spatial variability, their flexibility allows them to be integrated with vertical farming and the fact that they make renewable electricity available allows them to support controlled agriculture in urban areas (e.g., hydroponics, greenhouses), highlighting their potential as adaptable, multifunctional components of sustainable urban landscapes. UrAV can diversify income streams, increase resilience to extreme events, and attract non-traditional farmers (e.g., urban youth). In addition to the spatial and socio-economic factors considered in our city-scale scaling analysis, the influence of the urban heat-island (UHI) effect should also be taken into consideration when identifying suitable farming locations and when evaluating co-benefits. Incorporating UHI intensity maps or localized urban climate data would help refine site selection by capturing temperature-driven variability in crop performance, water demand, and heat stress risks across neighborhoods.

Methods

Agrivoltaics site description

The urban agrivoltaics system is located at the Ambler Field Station on the Ambler Campus of Temple University, Pennsylvania, USA (40°09′59″ N, 75°11′28″ W). The PV system was installed in April 2023 with minimal soil disturbance and became operational in May 2023. The system has a ~50 m^2 footprint and consists of 14 bifacial monocrystalline PV panels ($2.03 \times 1.00 \times 0.035$ m^3, 20.12% energy conversion efficiency). The PV panels are fixed (non-rotating), tilted to the south along their shorter sides, and elevated to a minimum and maximum clearance of 2.95 m and 3.33 m, respectively. Panels are laid out in 4 rows in a checkered design, with spaces between panels of 0.9 m and 0.40 m in the east-west and north-south directions, respectively (Fig. 1a).

After PV installation and operation, an environmental sensor network (Supplementary Fig. 9) was installed in two stages (2023 and 2024) and used to monitor the changes in microclimate between the agrivoltaics system and a neighboring plot under full sun conditions (control). The data were measured every 10 s and recorded every 5 min. Sensors (all from Campbell Scientific, Logan, UT) measured solar radiation (CS320-Digital Thermopile Pyranometer), air temperature (T) and relative humidity (RH; HygroVUE-TM 5-Temperature and Relative Humidity Sensor), wind speed and direction (MODEL 03002-5-Wind Sentry), precipitation (TE525-Series-Tipping Bucket Rain Gage), and soil moisture content and temperature (CS655-Water Content Reflectometer). Soil moisture sensors were placed at a 0.2 m depth, while the others were 2 m above the ground surface. Additional sensors for photosynthetic photon flux density (PPFD; CS310 Quantum PAR Sensor), ground-reflected radiation (SR05-L, ISO 9060 Second Class Pyranometer; one in the control and one in AV), and T/RH sensors, were placed at different heights and locations[33].

Instantaneous measurements of PAR (specifically, photosynthetic photon flux density, or PPFD; $n = 3$ per plot; 3 October 2024) and soil moisture content ($n = 4$ per plot; 24 September 2024) were made in all planting beds to capture the spatial variation in soil moisture and light transmittance throughout our sites. PPFD was measured with an LI-190SA quantum sensor connected to an LI-250A meter (both from LI-COR, Lincoln, NE) at two heights: 0.7 m (the height of basil, beans, radish, and lettuce) and at 2 m (the upper height of cherry tomatoes). Soil moisture was measured with a Hydrosense II (Campbell Scientific, Logan, UT). All PPFD measurements were made on a cloudy day and confined to a 45-min period when solar radiation was near its daily maximum (12:45–1:30 pm EDT). The transmittance ratio under the panels was computed based on a reference PPFD value measured for each bed in unshaded conditions. Average values from each plot were later interpolated across the site (using triangular interpolation) to gain insight into the spatial variability in light at both heights.

Crops were planted in elevated (or raised) crop beds, which are commonly used in urban farms to avoid soil toxicity issues. They were installed in March 2024; 8 beds were placed under the PV array and 4 in the control site. Each of the crop beds was 3.0 m L × 1.22 m W × 0.3 m H and had untreated wood frames. Cardboard was placed at the bottom of each bed to inhibit grass and weeds from penetrating into the overlying soil medium. The beds were filled with a blend of mushroom compost and screened topsoil (Primex Garden Center, Glenside, PA, USA). An additional compost layer (5 cm) was added later in the season to enhance nutrient availability[70]. Each bed was divided into 10 plots (each was 0.6×0.6 m^2; 2×2 ft^2) where five different crops (lettuce, cherry tomato, basil, bush bean, and radish; details about crops are found in Supplementary Table 8) were randomly assigned to plots such that none was duplicated in any column or row. Plots with lettuce, cherry tomato, bush bean, and radish were divided into two equal parts in the north-south direction to grow two varieties of each crop; this yielded subplots of 0.6×0.3 m^2 (2×1 ft^2) (Fig. 1a). In addition to the crop beds, six smaller beds (0.6×0.6 m^2; 2×2 ft^2) were installed for native species (aster, rudbeckia, royal catchfly, anise hyssop, obedient plant, and false sunflower; Supplementary Table 8) to increase pollination activity (Fig. 1a). From June through October 2024, all crop beds in the control and agrivoltaic sites were irrigated uniformly using an automated drip irrigation system (four lines ran across each bed).

Cultivation and measurements

All plants were propagated from seed (Johnny's Selected Seeds, Winslow, ME and W. Atlee Burpee Company, Warminster, PA). A single set of cherry tomatoes, beans, and basil plants was propagated and grown for the season, whereas lettuce and radishes were grown in multiple cycles. Tomato seeds were sown into trays in a greenhouse in March 2024 and transplanted into beds in May. Due to space limitations, one tomato plant of each variety was planted in each subplot, such that there were two per 0.6×0.6 m^2 plot. After 2 months, steel poles were installed to support the cherry tomato plants (since both varieties were indeterminate) at a maximum height of 1.5 m above the raised bed soil surface. Tomato fruits were harvested 17 times from July through November (i.e., almost weekly) and pruned monthly. Further, bush bean and basil seeds were sown directly into crop beds in April. Nine basil seeds and six seeds of each variety of beans were uniformly distributed in each plot or subplot. This would have yielded 9 basil plants and 12 bush bean plants from each variety in each plot if all had survived. Additionally, 10 lettuce plants and 20 radish plants of each variety were planted directly into each subplot during each cycle.

After each harvest, the fresh weight of the edible portions of plants was measured using a digital balance. This included mature bush bean and tomato fruits, whole lettuce heads, whole radish plants, and the largest ~90% of basil leaves (remaining leaves were not harvested). Morphological features, including the diameter of radish roots and cherry tomato fruits, the height of radish, cherry tomato, and lettuce plants, and the widest diameter of lettuce heads, were measured with calipers or rulers. Leaf areas of samples ($n = 1255$) of basil, both lettuce varieties, and both bush bean varieties were measured using an LI-3100C area meter (LI-COR, Lincoln, NE), and leaf dry masses were determined after drying for 72 h at 60 °C. Specific leaf area (SLA) was then computed as the ratio of leaf area to dry mass. In August, dry weights of samples ($n \approx 3$) of lettuce leaves, radish roots, cherry tomato fruits, bush bean fruits, and basil leaves were measured from each (sub)plot (drying was again for 72 h at 60 °C). These samples were later sent to Brookside Laboratories, Inc. (New Bremen, OH) for nutrient analysis, specifically concentrations of nitrogen, phosphorus, potassium, calcium, magnesium, sulfur, boron, iron, manganese, copper, zinc, and aluminum.

A component of leaf-level photosynthesis, specifically ETR, was measured in August and September 2024, typically between 10:00 and 14:00 EDT. For most varieties, measurements were made on each of two dates, though Stringless bush beans were measured on one date and French breakfast radish and Contender bush beans were not measured. For a given crop, three plants were typically measured from all occupied plots on the same day, though time constraints sometimes required omitting some plots. Given the 2:1 ratio of agrivoltaics vs. control beds, two measurements were made in agrivoltaics plots, alternating with measurements from one control plot. A pair of LI-600 Porometer/Fluorometers (LI-COR, Lincoln, NE) was used to record ETR and PPFD; this instrument does not allow for environmental control, so values reflect the agrivoltaic or control conditions during mid-day. The instrument was held at the angle of the leaf so PPFD measurements would reflect actual incident radiation.

Additionally, photosynthetic light response curves were recorded for one variety of each crop; this included Donato radish, Buttercrunch lettuce, Stringless bush bean, Supersweet tomato, and Genovese basil. ETR was thereby measured while PPFD was held at each of 9 light levels (spanning 0–2000 μmol/m^2/s) using an LI-6800F Portable Photosynthesis System (LI-COR, Lincoln, NE). Leaf temperatures, vapor pressure deficits, and chamber CO_2 levels were set to 25 °C, 1.5 kPa, and 400 ppm, respectively. Light curves were typically recorded from three control plants and six agrivoltaics plants of a single crop during a measurement day. A rectangular hyperbola was used to fit ETR values as a function of PPFD for each site and crop type (Eq. 29 from ref. 71). Lastly, energy production by the PV array was calculated based on the measured solar radiation and panel temperature[72].

Data analysis

Records of weights as well as morphological, physiological, and chemical measurements were organized in Excel spreadsheets and read into Jupyter lab notebooks, where Python was used to analyze the data. The main objective was to test the null hypothesis of no difference in means for each measurement and each crop type/variety. We used a Mixed-Effects Model in cases where the sample data was not normally distributed and a Linear Mixed-Effects Model in cases where the sample data was normally distributed (tested with Shapiro-Wilk tests; $\alpha = 0.05$). In both model types, there was a fixed effect for location (Agrivoltaics and Control), and random effects for crop bed and harvest date (i.e., they were set as blocks) while being grouped by subplot (row location in each crop bed). The hypotheses of no difference in means for each measurement were rejected when the p-value was below 0.1. Additionally, for the yields, all crop measurements were also pooled together and were subjected to a mixed-effects linear modeling, where the fixed effect was the Location, the measurements were grouped based on the crop type, and blocks were set as random effects, including harvest dates and bed crops.

Land equivalent ratio (LER) (Supplementary Table 4), which is widely used in agrivoltaics studies to assess land use efficiency, was used to assess the performance of our agrivoltaics system and was calculated by summing two ratios: (1) cumulative weights of crops in the agrivoltaics divided by that in the control and (2) estimated electricity production in the agrivoltaics divided by that produced in an equivalent land area with full-density panels[41]. The first ratio was calculated based on yield data measured throughout the growing season. Since the control site area had half the area of agrivoltaics site (25 vs. 50 m^2), we calculated the cumulative weights of crops over the growing season for both sites, and then we doubled the cumulative weights of the control. We summed the cumulative weights of all crops for each site and then computed the ratio. On the other hand, the second ratio was computed by dividing the optimum power capacity of the panels in our agrivoltaics design, which was comprised of 14 panels (each 410 W), by that of a hypothetical agrivoltaics design containing 28 full-density PV panels within the same area (50 m^2).

Food-energy spatial analysis

We performed a spatial analysis to evaluate the possibility of integrating urban agrivoltaics into vacant spaces in cities, including vacant lands and rooftops, which have been assessed as highly suitable for PV installations in places with limited space[73]. Accordingly, we chose Philadelphia, USA, due to its location in a temperate climate zone, its representation of typical cities facing common urban challenges (e.g., urban heat islands, food and energy inaccessibility), and its social and cultural heterogeneity. The city is also recognized for its abundance of green spaces (i.e., parks) and its flexibility to adopt urban agriculture. We examined the aerial coverage of regions where people have limited access to food and struggle to cover electricity bills. Shapefiles of food access, poverty distribution, and vacant spaces were obtained from OpenDataPhilly (https://opendataphilly.org/). We used ArcGIS Pro (ESRI, Redlands, CA) to find the intersection of regions with limited and no access to food with tracts having 40% or more people living under the poverty line. The resultant shapefile, which we characterize as food and energy deserts, was used to query the aerial coverage of intersected vacant lands and buildings and those located along a 0.5-mile buffer zone, considering 0.5 mile a maximum suitable walking distance[74]. In addition, population data were extracted from the US Census Bureau for the tracts included in the resultant shapefile that were used to approximate the number of households based on the average size of households in Philadelphia (2.48).

After determining the population data and areas of available land (vacant spaces) that could potentially be used for urban agrivoltaics, quantities of food, land, and energy were calculated. We considered a planetary health diet, the EAT-Lancet target intake for vegetables is 300 g/day on average[75,76] and a growing density of 2.785 kg/m^2 averaged across 5 different types of crops grown in raised beds[77]. Thus, we calculated the land needed to supply these regions, assuming that we need the land twice per year based on 2 growing seasons (every 6 months), adding 20% of additional land used for spacing between raised beds. Then, based on the capacity of the agrivoltaics site that we have in this study (5 kW in 50 m^2), we determined how much solar energy we could generate from the previously calculated land. To do this, we used the average annual consumption of a typical U.S. household, which is 10,791 kWh/yr according to the U.S. Energy Information Administration. To calculate the generated electricity from solar panels, we assumed that the agrivoltaics site generates energy at full capacity for 6 h (sunny hours usually range between 5 and 7). Limitations for the spatial analysis include calculating the area of vacant spaces that (1) is not affected by shade from neighboring tall buildings, and (2) is accessible to the grid, instead of using the gross area. Also, a challenge for this proposed strategy is the significant mass of soil that needs to be transported into the city to fill the raised beds to avoid toxicity issues, instead of using existing soils.

Data availability

The datasets generated and/or analyzed during the current study are not publicly available due to ongoing analyses but are available from the corresponding author upon reasonable request.

Received: 6 June 2025; Accepted: 17 March 2026;
Published online: 03 April 2026

References

1. Vilar-Compte, M. et al. Urban poverty and nutrition challenges associated with accessibility to a healthy diet: a global systematic literature review. *Int. J. Equity Health* **20**, 40 (2021).
2. Cornelsen, L. et al. What happens to patterns of food consumption when food prices change? Evidence from a systematic review and meta-analysis of food price elasticities globally. *Health Econ.* **24**, 1548–1559 (2015).
3. Gripper, A. B. et al. Community solutions to food apartheid: a spatial analysis of community food-growing spaces and neighborhood demographics in Philadelphia. *Soc. Sci. Med.* **310**, 115221 (2022).
4. Mishra, A. et al. Diminishing benefits of urban living for children and adolescents' growth and development. *Nature* **615**, 874–883 (2023).
5. Aris, I. M. et al. Birth outcomes in relation to neighborhood food access and individual food insecurity during pregnancy in the Environmental Influences on Child Health Outcomes (ECHO)-wide cohort study. *Am. J. Clin. Nutr.* **119**, 1216–1226 (2024).
6. FAO. Strengthening urban and peri-urban food systems to achieve food security and nutrition, in the context of urbanization and rural transformation. https://openknowledge.fao.org/handle/20.500.14283/cd1459en (2024).
7. Kohlhase, J. E. The new urban world 2050: perspectives, prospects and problems. *Reg. Sci. Policy Pract.* **5**, 153–166 (2013).
8. Skar, S. L. G. et al. Urban agriculture as a keystone contribution towards securing sustainable and healthy development for cities in the future. *Blue Green Syst.* **2**, 1–27 (2019).
9. Iida, A., Yamazaki, T., Hino, K. & Yokohari, M. Urban agriculture in walkable neighborhoods bore fruit for health and food system resilience during the COVID-19 pandemic. *npj Urban Sustain.* **3**, 1–10 (2023).
10. Tolazzi, A., Galli, N., Lobo Marchioni, D. M. & Rulli, M. C. Rethinking urban spaces to improve nutrition security through urban agriculture. *Earths Future* **13**, e2025EF006641 (2025).
11. Birdshire, K. R., Carper, A. L. & Briles, C. E. Bee community response to local and landscape factors along an urban-rural gradient. *Urban Ecosyst.* **23**, 689–702 (2020).

12. Puigdueta, I., Aguilera, E., Cruz, J. L., Iglesias, A. & Sanz-Cobena, A. Urban agriculture may change food consumption towards low carbon diets. *Glob. Food Secur.* **28**, 100507 (2021).
13. Ghanbari, M., Arabi, M., Georgescu, M. & Broadbent, A. M. The role of climate change and urban development on compound dry-hot extremes across US cities. *Nat. Commun.* **14**, 3509 (2023).
14. Moore, C. E. et al. The effect of increasing temperature on crop photosynthesis: from enzymes to ecosystems. *J. Exp. Bot.* **72**, 2822–2844 (2021).
15. IPCC. *Climate Change Mitigation, Agriculture*. https://archive.ipcc.ch/publications_and_data/ar4/wg3/en/ch8.html (2007).
16. Proctor, J., Rigden, A., Chan, D. & Huybers, P. More accurate specification of water supply shows its importance for global crop production. *Nat. Food* **3**, 753–763 (2022).
17. IPCC. *Technical Summary — Special Report on Climate Change and Land*. https://www.ipcc.ch/srccl/chapter/technical-summary/ (2019).
18. Rizwan, A. M., Dennis, L. Y. C. & Liu, C. A review on the generation, determination and mitigation of Urban Heat Island. *J. Environ. Sci.* **20**, 120–128 (2008).
19. Mora, C. et al. Global risk of deadly heat. *Nat. Clim. Change* **7**, 501–506 (2017).
20. Pantavou, K., Theoharatos, G., Mavrakis, A. & Santamouris, M. Evaluating thermal comfort conditions and health responses during an extremely hot summer in Athens. *Build. Environ.* **46**, 339–344 (2011).
21. Salamanca, F. et al. Assessing summertime urban air conditioning consumption in a semiarid environment. *Environ. Res. Lett.* **8**, 034022 (2013).
22. United Nations Department of Economic and Social Affairs. The Sustainable Development Goals Report 2025. New York (2025).
23. Ravi, S., Lobell, D. B. & Field, C. B. Tradeoffs and Synergies between biofuel production and large solar infrastructure in deserts. *Environ. Sci. Technol.* **48**, 3021–3030 (2014).
24. Ravi, S. et al. Colocation opportunities for large solar infrastructures and agriculture in drylands. *Appl. Energy* **165**, 383–392 (2016).
25. Choi, C. S. et al. Environmental co-benefits of maintaining native vegetation with solar photovoltaic infrastructure. *Earths Future* **11**, e2023EF003542 (2023).
26. Walston, L. J. et al. Examining the potential for agricultural benefits from pollinator habitat at solar facilities in the United States. *Environ. Sci. Technol.* **52**, 7566–7576 (2018).
27. Miskin, C. K. et al. Sustainable co-production of food and solar power to relax land-use constraints. *Nat. Sustain.* **2**, 972–980 (2019).
28. Edouard, S., Combes, D., Van Iseghem, M., Ng Wing Tin, M. & Escobar-Gutiérrez, A. J. Increasing land productivity with agriphotovoltaics: application to an alfalfa field. *Appl. Energy* **329**, 120207 (2023).
29. Zhang, B. et al. Deploying photovoltaic arrays in degraded grasslands is a promising win-win strategy for promoting grassland restoration and resolving land use conflicts. *J. Environ. Manag.* **349**, 119495 (2024).
30. Barron-Gafford, G. A. et al. Agrivoltaics provide mutual benefits across the food–energy–water nexus in drylands. *Nat. Sustain.* **2**, 848–855 (2019).
31. Othman, N. F. et al. Embracing new agriculture commodity through integration of Java Tea as high Value Herbal crops in solar PV farms. *J. Clean. Prod.* **91**, 71–77 (2015).
32. Jo, H. et al. Comparison of yield and yield components of several crops grown under agro-photovoltaic system in Korea. *Agriculture* **12**, 619 (2022).
33. Merheb, C. et al. Exploring micro-environmental conditions of urban agrivoltaics: Advancing sustainable green spaces and agriculture in temperate cities. *Sustain. Cities Soc.* https://doi.org/10.1016/j.scs.2025.107091 (2026).
34. Merheb, C., Macknick, J., Davatzes, N. & Ravi, S. Synergies and trade-offs of multi-use solar landscapes. *Nat. Sustain*. **8**, https://doi.org/10.1038/s41893-025-01600-1 (2025).
35. Macknick, J. et al. The 5 Cs of agrivoltaic success factors in the United States: lessons from the InSPIRE research study. https://doi.org/10.2172/1882930 (2022).
36. Merheb, C., Ravi, S. & Macknick, J. A global synthesis of multi-use solar energy projects: synergies and tradeoffs. In *AGU Fall Meeting Abstracts* Vol. 2023, GC21I–GC21039 (AGU, 2023).
37. Curioni, M., Galli, N., Manzolini, G. & Rulli, M. C. Global land-water competition and synergy between solar energy and agriculture. *Earths Future* **13**, e2024EF005291 (2025).
38. Campana, P. E. et al. Scientific frontiers of agrivoltaic cropping systems. *Nat. Rev. Clean Technol.* **1**, 801–821 (2025).
39. Sekiyama, T. & Nagashima, A. Solar sharing for both food and clean energy production: performance of agrivoltaic systems for corn, a typical shade-intolerant crop. *Environments* **6**, 65 (2019).
40. Weselek, A., Bauerle, A., Zikeli, S., Lewandowski, I. & Högy, P. Effects on crop development, yields and chemical composition of celeriac (Apium graveolens L. var. rapaceum) cultivated underneath an agrivoltaic system. *Agronomy* **11**, 733 (2021).
41. Valle, B. et al. Increasing the total productivity of a land by combining mobile photovoltaic panels and food crops. *Appl. Energy* **206**, 1495–1507 (2017).
42. Ko, J. et al. Simulation of crop yields grown under agro-photovoltaic panels: a case study in Chonnam Province, South Korea. *Energies* **14**, 8463 (2021).
43. Potenza, E., Croci, M., Colauzzi, M. & Amaducci, S. Agrivoltaic system and modelling simulation: a case study of soybean (Glycine max L.) in Italy. *Horticulturae* **8**, 1160 (2022).
44. Lee, H. J., Park, H. H., Kim, Y. O. & Kuk, Y. I. Crop cultivation underneath agro-photovoltaic systems and its effects on crop growth, yield, and photosynthetic efficiency. *Agronomy* **12**, 1842 (2022).
45. Jiang, S. et al. Effects of different photovoltaic shading levels on kiwifruit growth, yield and water productivity under "agrivoltaic" system in Southwest China. *Agric. Water Manag.* **269**, 107675 (2022).
46. Ferrara, G., Boselli, M., Palasciano, M. & Mazzeo, A. Effect of shading determined by photovoltaic panels installed above the vines on the performance of cv. Corvina (Vitis vinifera L.). *Sci. Hortic.* **308**, 111595 (2023).
47. Ramos-Fuentes, I. A. et al. Effects of shade and deficit irrigation on maize growth and development in fixed and dynamic AgriVoltaic systems. *Agric. Water Manag.* **280**, 108187 (2023).
48. Moon, H.-W. & Ku, K.-M. The effect of additional shading utilizing agriphotovoltaic structures on the visual qualities and metabolites of broccoli. *Front. Plant Sci.* **14**, 1111069 (2023).
49. USDA ERS - Common Ground for Agriculture and Solar Energy: Federal Funding Supports Research and Development in Agrivoltaics. https://www.ers.usda.gov/amber-waves/2024/april/common-ground-for-agriculture-and-solar-energy-federal-funding-supports-research-and-development-in-agrivoltaics/.
50. Rabb, R. C. M. Rabb resolution to study agrivoltaic farming approved by PA House Local Government Committee. https://www.pahouse.com/InTheNews/NewsRelease/?id=131508 (2023).
51. Merheb, C., Phuyal, P., Caplan, J., Macknick, J. & Ravi, S. Effect of an Urban Agrivoltaics System on Various Crops in a Temperate Climate. In *AGU Fall Meeting Abstracts* Vol. 2024 (AGU, 2024).
52. Semeraro, T. et al. Shading effects in agrivoltaic systems can make the difference in boosting food security in climate change. *Appl. Energy* **358**, 122565 (2024).
53. Stagnari, F. et al. Light quantity and quality supplies sharply affect growth, morphological, physiological and quality traits of basil. *Ind. Crops Prod.* **122**, 277–289 (2018).
54. Yamori, W., Hikosaka, K. & Way, D. A. Temperature response of photosynthesis in C3, C4, and CAM plants: tempera ture acclimation and temperature adaptation. *Photosynth. Res.* **119**, 101–117 (2013).
55. Katul, G. Agrivoltaics in color: going from light spectra to biomass. *Earths Future* **11**, e2023EF003512 (2023).

56. Bhattacharya, A. Effect of low-temperature stress on germination, growth, and phenology of plants: a review. In *Physiological Processes in Plants Under Low Temperature Stress* (ed. Bhattacharya, A.) 1–106 https://doi.org/10.1007/978-981-16-9037-2_1 (Springer, 2022).
57. Reed, R. C., Bradford, K. J. & Khanday, I. Seed germination and vigor: ensuring crop sustainability in a changing climate. *Heredity* **128**, 450–459 (2022).
58. Mueller, K. E., Kray, J. A. & Blumenthal, D. M. Coordination of leaf, root, and seed traits shows the importance of whole plant economics in two semiarid grasslands. *New Phytol.* **241**, 2410–2422 (2024).
59. Epstein, E., Bloom, A. J. *Mineral Nutrition of Plants: Principles and Perspectives* (Oxford University Press, 2004).
60. Hawkesford, M. J. & De Kok, L. J. Managing sulphur metabolism in plants. *Plant Cell Environ.* **29**, 382–395 (2006).
61. Astolfi, S., Celletti, S., Vigani, G., Mimmo, T. & Cesco, S. Interaction between sulfur and iron in plants. *Front. Plant Sci*. **12**, 670308 (2021).
62. Schmidt, S. B., Jensen, P. E. & Husted, S. Manganese deficiency in plants: the impact on photosystem II. *Trends Plant Sci.* **21**, 622–632 (2016).
63. Hawson, M. Manganese deficiency in vegetables. https://www.agric.wa.gov.au/vegetables/manganese-deficiency-vegetables (2016).
64. Brdar-Jokanović, M. Boron toxicity and deficiency in agricultural plants. *Int. J. Mol. Sci.* **21**, 1424 (2020).
65. Wintz, H., Fox, T. & Vulpe, C. Responses of plants to iron, zinc and copper deficiencies. *Biochem. Soc. Trans.* **30**, 766–768 (2002).
66. Rydzewski, C., Merheb, C., Macknick, J. & Ravi, S. Evaluating the environmental co-benefits and tradeoffs of urban agrivoltaics in Philadelphia. In *Proc. AGU Fall Meeting Abstracts* Vol. 2023, GC21I–GC21045 (2023).
67. Mayer, V. L., Hillier, A., Bachhuber, M. A. & Long, J. A. Food insecurity, neighborhood food access, and food assistance in Philadelphia. *J. Urban Health* **91**, 1087–1097 (2014).
68. Colelli, F. P., Wing, I. S. & Cian, E. D. Air-conditioning adoption and electricity demand highlight climate change mitigation–adaptation tradeoffs. *Sci. Rep.* **13**, 4413 (2023).
69. Vicedo-Cabrera, A. M. et al. The burden of heat-related mortality attributable to recent human-induced climate change. *Nat. Clim. Change* **11**, 492–500 (2021).
70. Merheb, C. & Chatila, J. Assessment of physical and structural properties of straw residues and chicken manure used as organic additives in agricultural soils. *J. Soil Sci. Plant Nutr.* **23**, 5312–5323 (2023).
71. Busch, F. A. et al. A guide to photosynthetic gas exchange measurements: Fundamental principles, best practice and potential pitfalls. *Plant Cell Environ.* **47**, 3344–3364 (2024).
72. Zonato, A. et al. Exploring the effects of rooftop mitigation strategies on urban temperatures and energy consumption. *J. Geophys. Res. Atmos.* **126**, e2021JD035002 (2021).
73. Merheb, C. Why should imminent international funds for solar photovoltaics go to families and the private sector and not to the government to stop the electricity crisis in Lebanon? *Energy Policy* **192**, 114223 (2024).
74. Yang, Y. & Diez-Roux, A. V. Walking distance by trip purpose and population subgroups. *Am. J. Prev. Med.* **43**, 11–19 (2012).
75. Willett, W. et al. Food in the anthropocene: the EAT–Lancet Commission on healthy diets from sustainable food systems. *Lancet* **393**, 447–492 (2019).
76. Ali, Z. et al. Adherence to EAT-Lancet dietary recommendations for health and sustainability in the Gambia. *Environ. Res. Lett.* **17**, 104043 (2022).
77. Miernicki, E. A., Lovell, S. T. & Wortman, S. E. Raised beds for vegetable production in urban agriculture. *Urban Agric. Reg. Food Syst.* **3**, 180002 (2018).

Acknowledgements

This study was funded by the National Science Foundation to S. Ravi (CAREER Award #1943969) and the InSPIRE project through the U.S. Department of Energy Office of Energy Efficiency and Renewable Energy (EERE) Solar Energy Technologies Office under award DE-EE00034165 to J. Macknick. The funder played no role in study design, data collection, analysis and interpretation of data, or the writing of this manuscript. The authors gratefully acknowledge the support of Temple University staff and faculty in the installation and operation of the agrivoltaics test site at the Ambler Field Station. Special thanks go to Mr. Minh Nguyen (Senior Business Manager, Department of Earth and Environmental Science), Mr. Kevin Orangers (Deputy Director, Temple University Ambler), Dr. Brent Sewall (Director, Ambler Field Station), Dr. Mariana Bonfim (Managing Director, Ambler Field Station), and Mr. Joseph Imszennik (Facilities Manager, Temple University Ambler) for their valuable assistance. The authors thank Mr. Todd Baylson and Mr. Micah Gold-Markel (Solar States) for their essential contributions in designing and developing the solar infrastructure used in this study. We also thank Anrui Xu (Radnor High School) and Veronica Mafla Hernandez (undergraduate student, Temple University) for their contributions to data collection and Dr. Thomas Mozdzer (Biology Professor, Bryn Mawr College) for loaning his LI-600 instruments.

Author contributions

Conceptualization: C.M., S.R., and J.S.C. Data curation: C.M. Methodology: C.M., S.R., P.P., J.M. N.C.D., and J.S.C. Formal analysis: C.M. Writing—original draft: C.M. Writing—review and editing: C.M., S.R., J.S.C., J.M., and N.C.D. Supervision: S.R. Project administration: S.R. Funding acquisition: S.R. and J.M.

Competing interests

The authors declare no competing interests.

Additional information

Supplementary information The online version contains supplementary material available at https://doi.org/10.1038/s42949-026-00381-6.

Correspondence and requests for materials should be addressed to Sujith Ravi.